Turkish Journal of Electrical Engineering & Computer Sciences

http://journals.tubitak.gov.tr/elektrik/

Research Article

Turk J Elec Eng & Comp Sci
(2017) 25: 4254 – 4267

doi:10.3906/elk-1612-84

Creation of a dynamic model of the electrification and traction power system of a 25 kV AC feed railway line together with analysis of different operation scenarios using MATLAB/Simulink

İlhan KOCAARSLAN[1], Mehmet Taciddin AKÇAY[2], Sırrı Erdem ULUSOY[3], Emrah BAL[3], Hasan TİRYAKİ[1,*]

[1]Department of Electrical and Electronics Engineering, Faculty of Engineering, İstanbul University, İstanbul, Turkey
[2]İstanbul Metropolitan Municipality, Directorate of Rail Systems, İstanbul, Turkey
[3]Are Engineering, İstanbul, Turkey

Received: 07.12.2016 • **Accepted/Published Online:** 19.04.2017 • **Final Version:** 05.10.2017

Abstract: In this study, the simulation of an electrification system and traction power system of a 25 kV AC feed railway line was performed with all its subcomponents using MATLAB/Simulink. The power flow theory was used while modeling the railway electrification system. The transformer substation, catenary, rail, and vehicle were modeled together with the operational data. This model is used in order to determine the number of transformers, the distance of feeding centers, and the frequency of trips. The optimum design of electrification projects depends on these criteria. A dynamic structure was created with a new algorithm developed for vehicle load characteristics. The simulation of the electrification system and traction power system is performed before the analysis stage, together with the vehicle and other design parameters. This analysis is performed for the best performance of the systems. In this study, the power simulation of the railway was conducted for three different operation scenarios using MATLAB/Simulink.

Key words: Electrification, line, power flow, railway, traction power

1. Introduction

The limits of carbon emission cause a decrease in fossil fuels and the proliferation of electric transportation systems [1]. Energy consumption may reach critical values in railways as a result of the use of high-power equipment. High power consumption causes power quality problems in the electrical system [2]. Various power compensators are used for this problem [3]. Voltage fluctuation affects the voltage of the load bar and the supply voltage [4]. While designing a railway electrification system, it is aimed to supply the necessary energy that is required by vehicles. The number of vehicles to be used is determined using a feasibility analysis report. The traction power system is designed after this analysis. The alternating current and direct current systems can be used in the railway electrification system design. The line voltage is determined using this simulation based on the slope, curve, vehicle specification, and vehicle consumption. The traction power supply voltages used in railway applications are shown in Table 1.

While 25 kV AC supply voltage is used in long-distance railways, 750 V DC and 1500 V DC supply voltages are used in urban railway lines. In AC railways, the Y-D11 transformer and Scott transformer can be used as a traction transformer [5]. A 2 × 25 kV AC feeding system has certain advantages when compared to

*Correspondence: hasan.tiryaki@istanbul.edu.tr

Table 1. Supply voltage of traction systems (TS EN 50163).

Electrification system	Lowest nonpermanent voltage	Lowest permanent voltage	Nominal voltage	Highest permanent voltage	Highest nonpermanent voltage
15 kV AC 16.7 Hz	11 kV AC	12 kV AC	15 kV AC	17.25 kV AC	18 kV AC
25 kV AC 50 Hz	17.5 kV AC	19 kV AC	25 kV AC	27.5 kV AC	29 kV AC

other AC feeding systems [6]. Network frequencies of 50 Hz and lower are used in AC railways [7]. The power flow analysis, electrification system, and traction power system simulation are performed after determining the catenary supply voltage. The power consumption curve is examined based on the movement of the vehicle for the optimum power system design. The variety of vehicle models, dynamic load state, operational problems, and the determination of the places of substations make this simulation more complex and more difficult [8]. Catenary voltage and current, vehicle voltage, flow, and other electrical data are analyzed with this simulation. This simulation and power flow calculations are important for the railway operation performance [9]. Vehicle specifications, line parameters, operational data, constraints of the system, and data on the rail system network are used in this simulation.

2. AC feeding railway model

AC railways mainly use a 25 kV 50 Hz electric system. In this type of supply, the single phase system is connected to the three-phase system [10]. In the AC system 50 km feeding zones are created for a possible phase overlap problem. These zones are called neutral zones. Neutral zones are fed from different points [11]. The length of these zones varies between 60 and 120 m [12]. The 154 kV phase–phase voltage of the interconnected system is turned into 25 kV phase-neutral supply voltage in transformer stations. In AC and DC railways, rails are used for traction power return current [13]. Two traction power transformers are used in substations.

The equivalent circuit of an AC railway is shown in Figure 1. AC railway equivalent circuit equations are shown with Eq. (1). Z1 and Z3 mean catenary and rail impedances. These values vary with the position of the vehicle. V1 represents the voltage of the vehicle and Vn1 represents the nominal source voltage. $I_{vehicle}$ is the vehicle's current. The maximum vehicle power may rise up to 20 MVA in railways that consume high power [14].

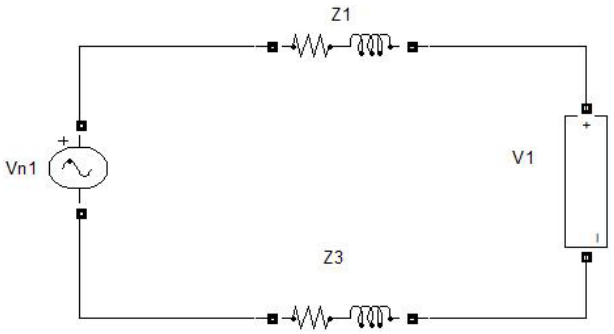

Figure 1. Equivalent circuit model of AC railway.

$$V_1 = V_{n1} - I_{vehicle} \times Z_1 - I_{vehicle} \times Z_3 \tag{1}$$

Electrical losses and voltage drop depend on the number of supply centers and the performance of the power

system [15]. The vehicle includes a traction system transformer, three-phase PWM inverter, and asynchronous engine [16]. The asynchronous engine may generate electricity by working as a generator during regenerative braking [17]. New traction power converters and other device equipment are developed with the advancement of technology and new studies [18].

A single-line diagram of the supply system in the transformer station of an AC railway is shown in Figure 2. There is more than one supply point in each transformer station for the continuity of operation [19]. When a transformer station collapses, another transformer station can supply the system.

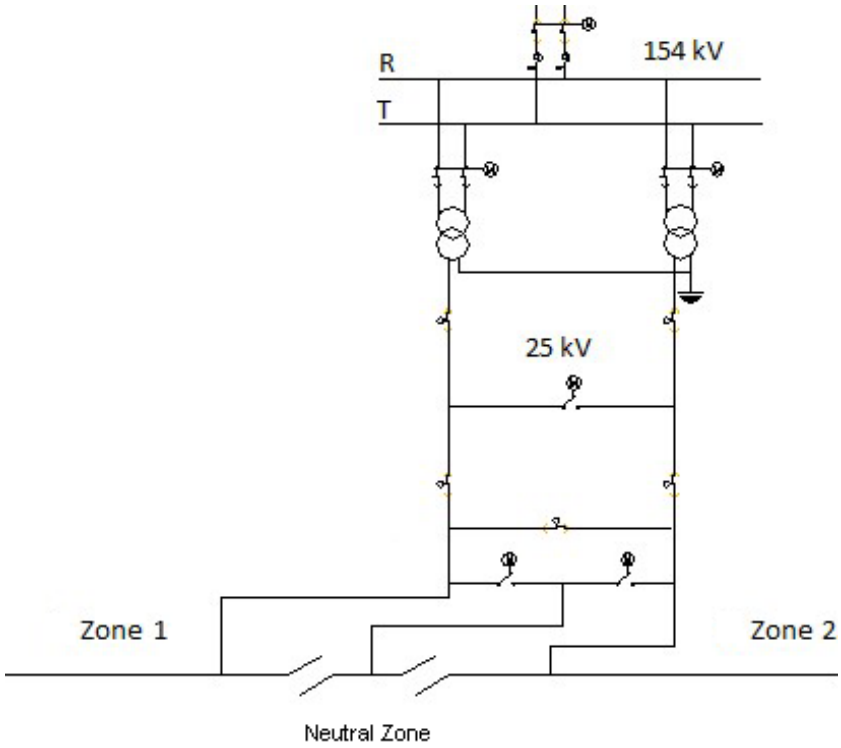

Figure 2. Single line diagram of substation.

$$P_{vehicle} = V_1 \times I_{vehicle} \tag{2}$$

The direction of the power flow from supply points to the vehicle is shown in Figure 3. Points 1 and 3 show the supply points, while point 2 shows the point where the vehicle is located. Bar Y is shown by the admittance matrix (3). Eqs. (4) and (5) show the Newton–Raphson power flow equations.

$$Y = \begin{bmatrix} Y_{11} & Y_{12} & Y_{13} \\ Y_{21} & Y_{22} & Y_{23} \\ Y_{31} & Y_{32} & Y_{33} \end{bmatrix} \tag{3}$$

$$P_i = V_i \times \sum_{j=1}^{i} V_j Y_{ij} \tag{4}$$

$$\begin{bmatrix} P_i \\ P_j \end{bmatrix}^{n+1} = \begin{bmatrix} P_i \\ P_j \end{bmatrix}^{n} + \begin{bmatrix} \frac{\partial P_i}{\partial V_i} & \frac{\partial P_i}{\partial V_j} \\ \frac{\partial P_j}{\partial V_i} & \frac{\partial P_j}{\partial V_j} \end{bmatrix} \begin{bmatrix} V_i^{n+1} & V_i^{n} \\ V_j^{n+1} & V_j^{n} \end{bmatrix} \tag{5}$$

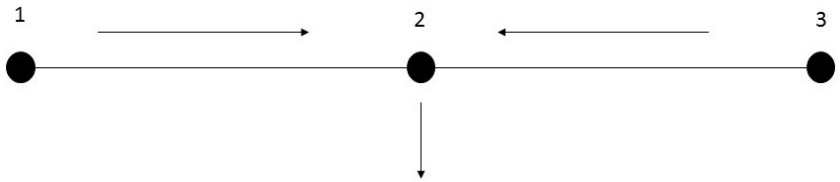

Figure 3. Power transmission.

The power system is designed according to this equation and calculations. The determination of the supply points and the number of vehicles is performed after this. The catenary voltage and vehicle voltage depend on the movement of the vehicle [20]. The input and output data of the system are given in Figure 4. The model of the system consists of number of vehicles, traction power, curve resistance, grade resistance, and line voltage as shown in the figure.

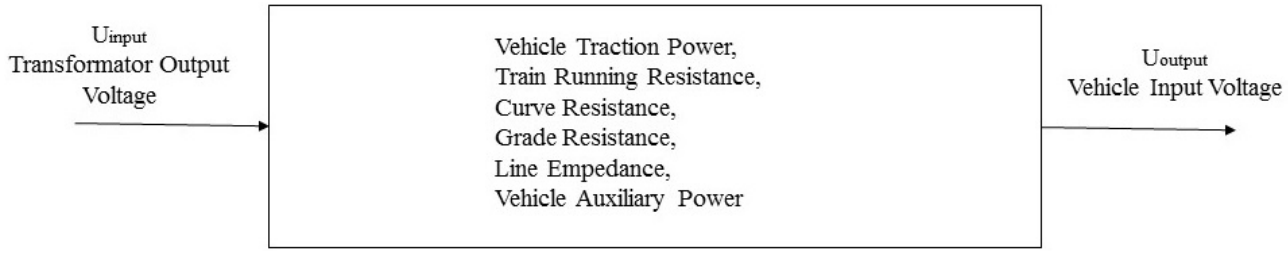

Figure 4. Model of system.

3. Simulation model

The model of the railway power system consists of certain steps. These are obtaining certain data based on the equivalent circuit design, vehicle model, transformer station model, and vehicle operation [21]. The vehicle model is quite critical for the system analysis in simulation [22]. In the literature there are railway power flow studies and electrification system simulations. However, in this study, a dynamic model is created with a new algorithm for the vehicle acceleration mode, permanent speed mode, and braking mode. With this algorithm vehicle movement is modeled dynamically and simultaneously depending on environmental effects and vehicle load characteristics. Vehicle speed profile is created simultaneously. In this way real vehicle characteristics are obtained and the simulation performance is increased. The electrification system analysis is done for the transformator station loss depending on the trip frequency.

3.1. Algorithm developed for different vehicle driving modes

Railway power system calculations are critical for the system analysis [23]. All operational data and line parameters are included in these calculations. The vehicle model is created with vehicle movement equations [24]. The curve resistance, slope resistance, and movement resistance depend on the movement of the vehicle [25]. The vehicle equations are presented below. Rotational mass is calculated with Eq. (6) with the help of coefficient ξ. This coefficient corresponds to 5% of the vehicle mass. M means the vehicle mass, while m' means the rotational mass.

$$m = \xi \times m \tag{6}$$

The total force that affects the vehicle is shown by F_i (7) equation, in which a means the acceleration.

$$\sum_{i=1}^{n} F_i = m' \times a \tag{7}$$

Fr, Fgr, and Fc mean the vehicle movement resistance force, slope resistance force, and curve resistance force and are shown with Eqs. (8), (9), and (10), respectively. The traction force is presented by (11).

$$F_r = a + Bv + Cv^2 \tag{8}$$

$$F_{gr} = mgsin(a) \tag{9}$$

$$F_c = (mg \div 1000) \times ((C_1 - C_2R) \div (R - C_3)) \tag{10}$$

$$F_{trac} = F_r + F_{gr} + F_c \tag{11}$$

The power calculation is shown with Eq. (12).

$$P_{vehicle} = F \times V \tag{12}$$

The vehicle consumes electrical power during acceleration and gives power to the system during braking [26]. This power can be used by other vehicles or the transformer station [27]. Figure 5 shows the traction force–speed graph of the Turkish State Railways (TCDD) ROTEM vehicle with a power of 5 MVA [28]. The current control signal is calculated with the above equations. The design for the vehicle acceleration and braking modes is performed according to the traction force curve shown in Figure 5. The red line is used at speeds that are lower than 73 km/h. The black line is used at speeds that are higher than 73 km/h. Point 0 corresponds to the reference point of the graph. The vehicle acceleration algorithm is shown in Figure 6. The vehicle power consumption and other electrical parameters are calculated with this algorithm. Part I is the first part of the red line. This part is the constant force part. Part II is the remaining part of the red line. Part III is the black line, and it starts at the end of the red line. The vehicle braking mode is indicated by the blue line in Figure 5. Part I is the part where the vehicle speed is higher than 133 km/h. Part II is the remaining part of the line. The braking algorithm is shown in Figure 7. As shown in Figure 8, the vehicle is modeled as a controlled current source. The control signal of the current to be generated in cases of acceleration and braking is calculated with these algorithms. The voltmeter is used to obtain the values of the measurement block vehicle voltage and catenary voltage. The generation of the vehicle control signal is shown in Figure 9. The speed limits, slope, curve, switch placements, and other line properties are important for this signal. With this model, the signals of the vehicle acceleration mode, nominal speed mode, and braking mode are calculated.

3.2. The model of AC railway transformer station

The model of the transformer station is shown in Figure 10. In transformer stations, 154 kV phase–phase voltage is turned into 25 kV phase-neutral single phase voltage. Feeder and return cables are modeled as an R-L component. The ammeter measurement block was used for obtaining the feeder current values of the transformers.

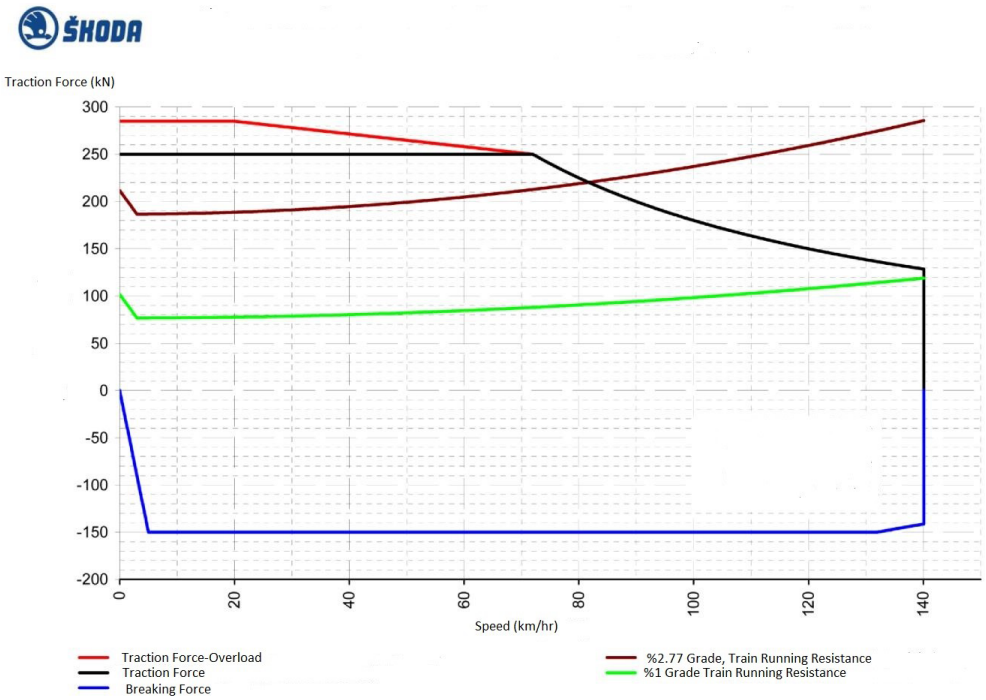

Figure 5. Graphic of vehicle traction force speed.

3.3. Modeling of the catenary and rail

The catenary and rail are modeled as an R-L component. This model is shown in Figure 8. This model includes the carrier conductor, contact conductor, and rail.

4. The model of the railway used

For the electrification system 25 kV 50 Hz AC supply voltage is used. There are two 154 kV/25 kV transformers in each transformer station for the continuity of operation. The traction power system allows trip frequency of 25 min and 50 min. Twenty vehicles are used for the vehicle traffic. While 10 vehicles move in a direction that is from the start to the end of the line, the other 10 vehicles move in the opposite direction.

5. The modeling of the Afyon–Manisa railway with MATLAB

The Afyon–Manisa railway is 355 km long and consists of 35 stations and 6 transformer stations. The transformer stations are at 35, 95, 155, 215, 275, and 335 km along the line. Each transformer station is modeled with a MATLAB/Simulink model. The line that covers the catenary and rail consists of 7 MATLAB blocks. The vehicle operation is performed with 20 vehicles at the trip frequency of 25 min and 10 vehicles at the trip frequency of 50 min. While 10 of the 20 vehicles start off from Manisa, the other 10 vehicles start off from Afyon at the trip frequency of 50 min and while 5 of the 10 vehicles start off from Manisa, the other 5 vehicles start off from Afyon at the trip frequency of 50 min. A trip frequency of 25 min and 50 min was determined. "ts" sampling time was selected as 1e-3 for the simulation. Tp is the simulation duration and includes the operation period of a vehicle enterprise. The datasheets of the Afyon–Manisa line were used for the simulation parameters.

The catenary impedance is 174 + 390 j mΩ/km, feeder cable impedance is 0.103 + 0.266 j ohm/km and

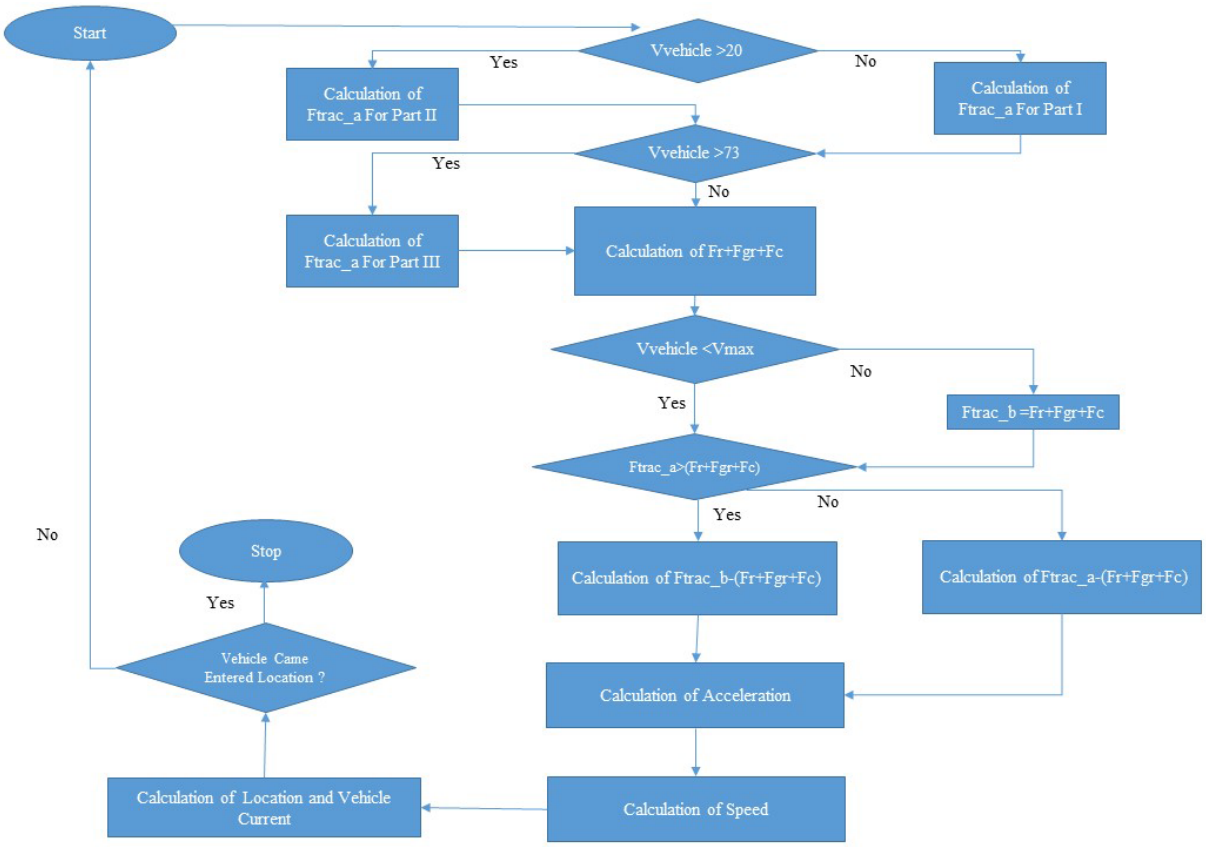

Figure 6. Vehicle acceleration algorithm.

transformer impedance is $0.151 + j \cdot 3.778\ \Omega$. The simulation screen and simulation flow scheme are shown in Figures 11 and 12.

6. The analysis of different operation scenarios

Certain problems can be encountered in the electrification system during the vehicle traffic in the enterprise. The most critical among these is the loss of a transformer station. This problem affects the vehicle traffic. The state of losing a transformer station is studied especially through simulation before the process of construction. The speed profile of the trains is given in Figure 13.

6.1. Nominal operation state at the trip frequency of 25 min

The nominal operation state shows that all transformer stations operate smoothly at a specified trip frequency. The simulation results of the Afyon–Manisa railway line for the trip frequency of 25 min are presented in Figure 14. In Figures 14–19, * and + represent the locations of the train stations and transformer stations. The locations of the disabled transformer stations are shown in black in Figures 16–19. The minimum catenary voltage varies between 21.8 kV and 25 kV. The lowest voltage of 21.8 kVs is observed between 200 and 250 km. These values are within the limits of the traction supply voltage standards. In this state there are 20 trains in the system. The lowest minimum catenary voltages are mostly seen at the points remote from transformer stations.

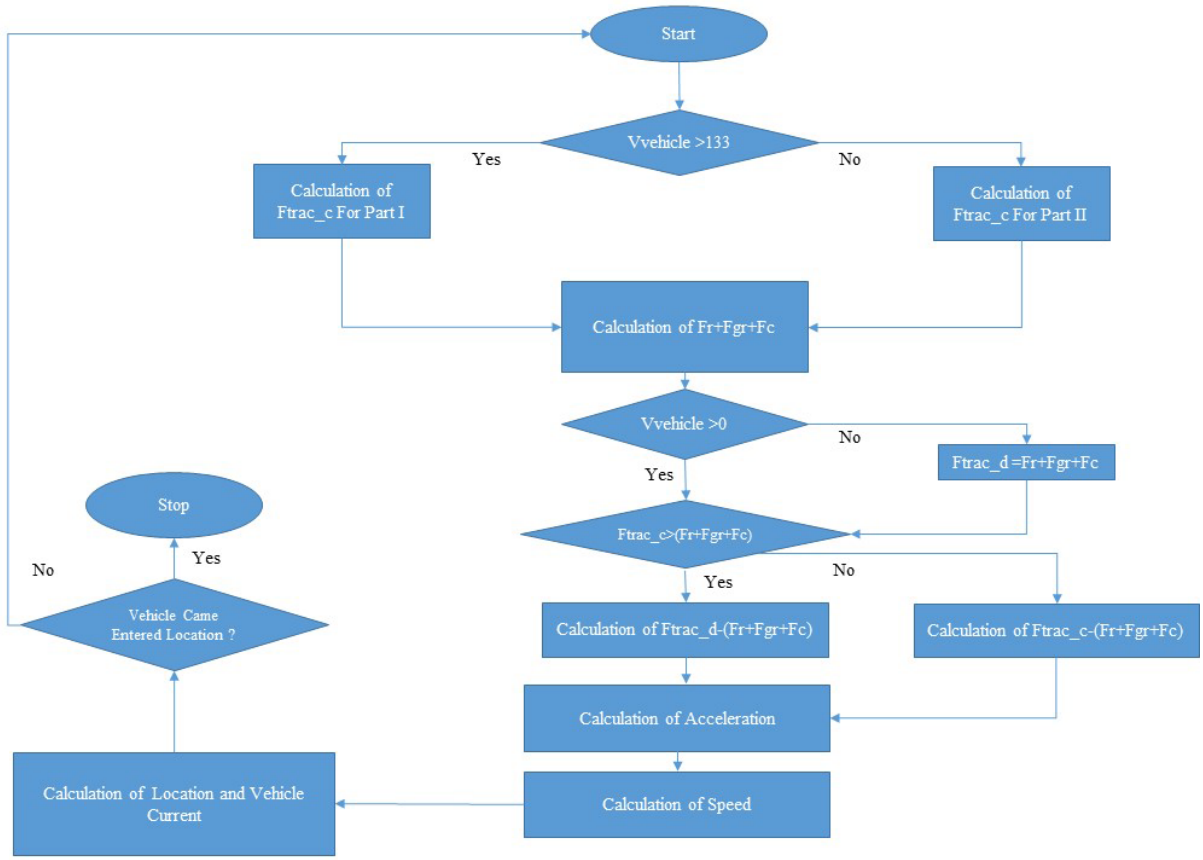

Figure 7. Vehicle breaking algorithm.

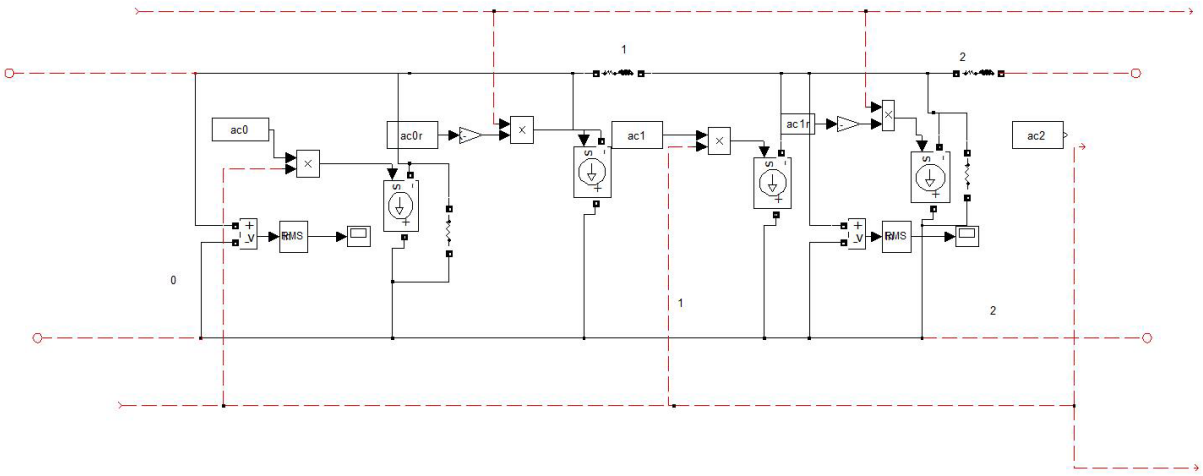

Figure 8. Vehicle model.

6.2. Nominal operation state at the trip frequency of 50 min

Figure 15 shows the simulation results of the trip frequency of 50 min and the nominal operation state. The minimum catenary voltage varies between 22.1 kV and 25 kV. The lowest catenary voltage of 22.1 kV gains this value by the end of 200 km as seen in Figure 15. The minimum catenary voltage rises at transformer station

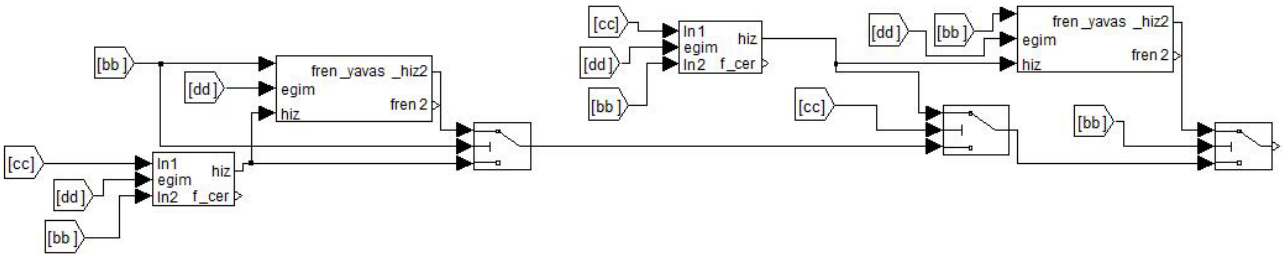

Figure 9. Model of vehicle control signal.

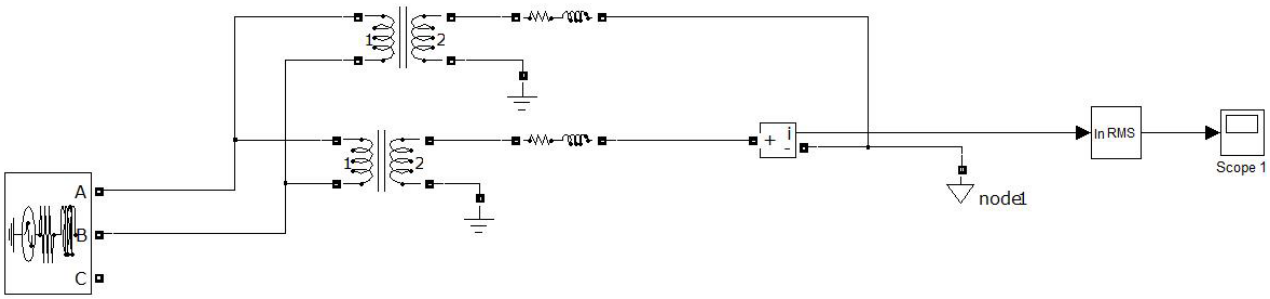

Figure 10. Model of substation.

feeding points. The lowest catenary voltage that occurs in this state is higher than the values that occur at the trip frequency of 25 min. In this state there are 10 trains in the system.

6.3. The state of losing the first transformer station at the trip frequency of 25 min

The state of losing the first transformer station located 35 km along the line of the electrification system was examined. In this case, the second transformer station feeds the region that was fed by the first. The minimum catenary voltage occurs in the region of the first transformer station as seen in Figure 16. The minimum catenary voltage is 14 kV and is also shown in Figure 16. This value is critical as it is beyond the traction supply voltage standards. There are 20 trains in the system during the incident.

6.4. The state of losing the first transformer station at the trip frequency of 50 min

The minimum catenary voltage in the state when the power system is operated at the trip frequency of 50 min is shown in Figure 17. In this case, the minimum catenary voltage is 19.5 kV, and this value is within the limits of the standard. There are 10 trains in the system during the incident. The lowest catenary voltage of 19.5 kV gains this value by the end of 15 km as seen in Figure 17.

6.5. The state of losing the second transformer station at the trip frequency of 25 min

The state of losing the second transformer station located 95 km along the line of the electrification system was examined. In this case, the first and third transformer stations feed the region that was fed by the second. The minimum catenary voltage occurs in the region of the second transformer station as seen in Figure 18. The minimum catenary voltage is 18 kV and is also shown in Figure 18. This value is critical as it is beyond the traction supply voltage standards. There are 20 trains in the system during the incident.

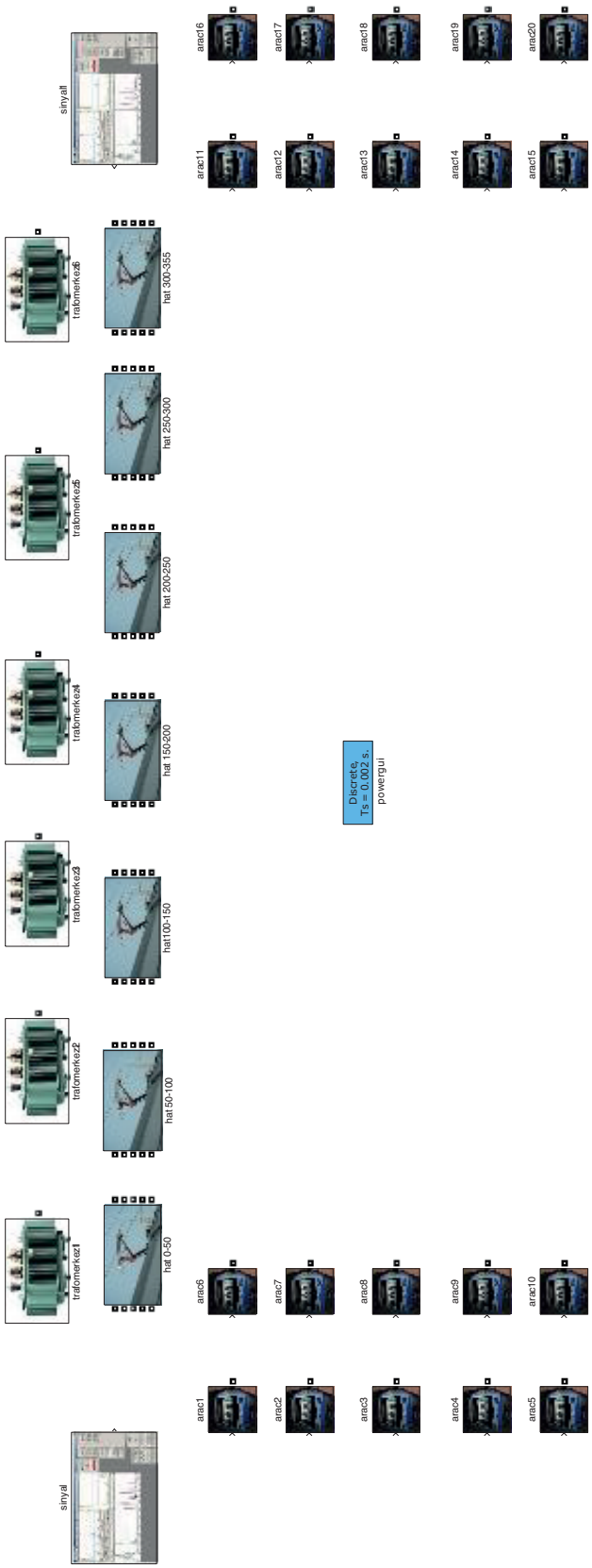

Figure 11. MATLAB screen of power simulation.

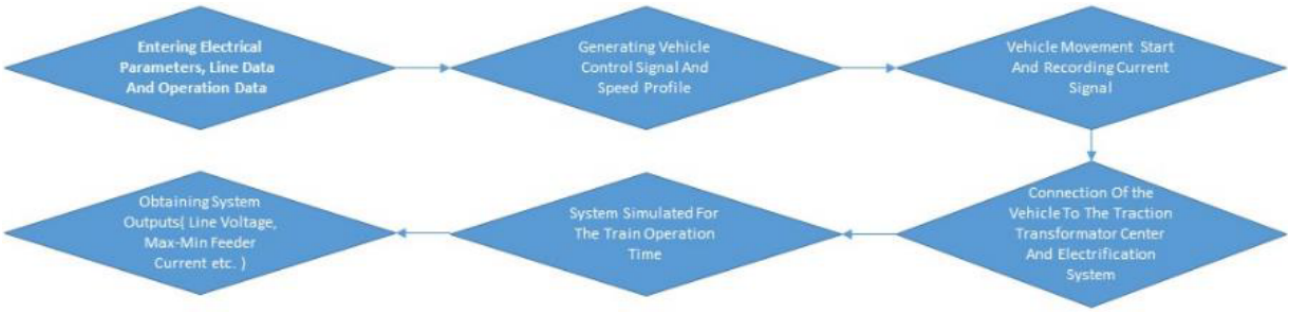

Figure 12. Flow chart of simulation.

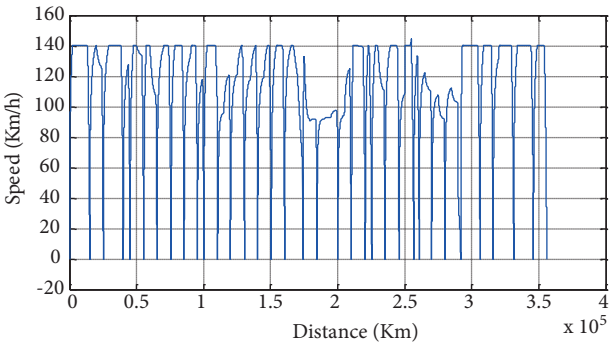

Figure 13. Speed profile of trains.

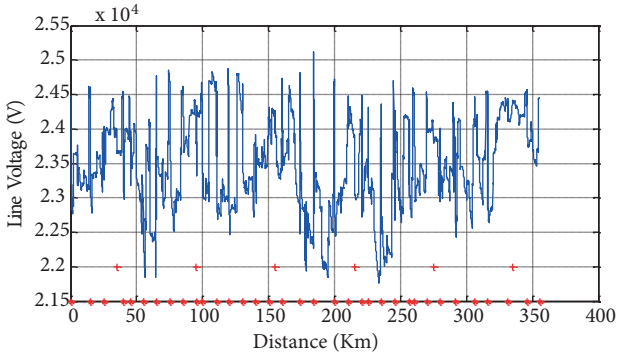

Figure 14. Catenary line voltage for nominal operation with 25 min headway.

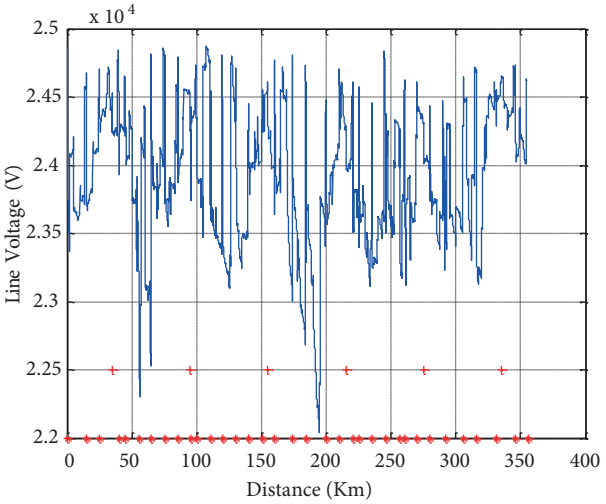

Figure 15. Catenary line voltage graphic for nominal operation with 50 min headway.

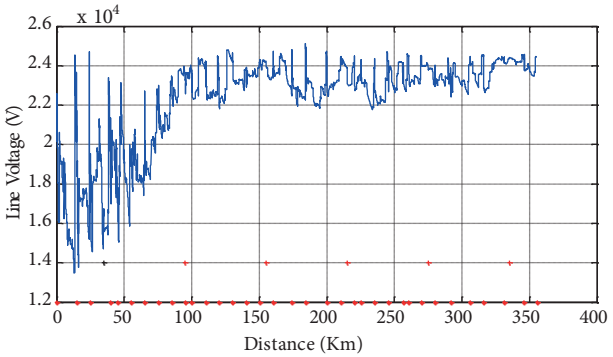

Figure 16. Catenary line voltage graphic for the loose of first substation with 25 minutes headway.

6.6. The state of losing the second transformer station at the trip frequency of 50 min

The minimum catenary voltage in the state when the power system is operated at the trip frequency of 50 min is shown in Figure 19. In this case, the minimum catenary voltage is 20 kV, and this value is within the limits of the standard. There are 10 trains in the system during the incident. The lowest catenary voltage of 20 kV gains this value by the end of 65 km as seen in Figure 19.

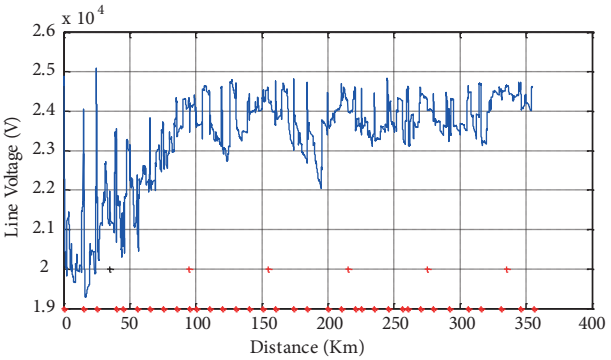

Figure 17. Catenary line voltage graphic for the loss of the first substation with 50 min headway.

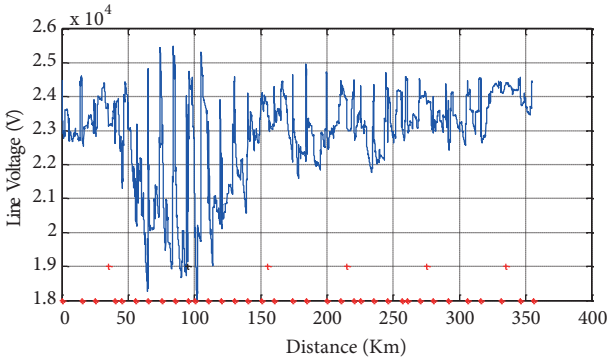

Figure 18. Catenary line voltage graphic for the loss of the second substation with 25 min headway.

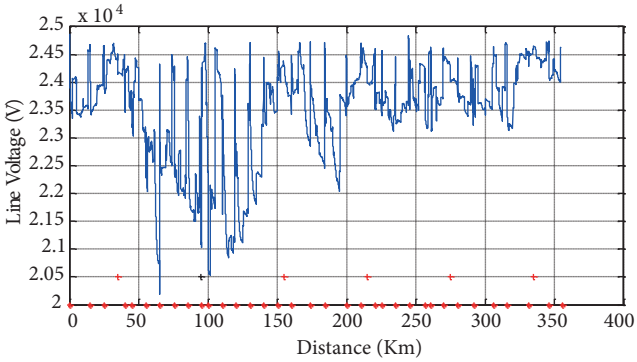

Figure 19. Catenary line voltage graphic for the loss of the second substation with 50 min headway.

7. Conclusion

In this study, the simulation of the electrification system and the traction power system of the 25 kV 50 Hz AC feeding Afyon–Manisa railway line was performed according to different operation scenarios using MATLAB/Simulink. More effective operation conditions were investigated depending on the traction supply voltage standard and minimum catenary voltage. The situations that occur under different operation conditions and solution suggestions for operation continuity are summarized in Table 2. In the normal operation, 20 trains can move in the system at the trip frequency of 25 min and 10 trains can move at the trip frequency of 50 min. During the transformer station incident 10 trains can move at the trip frequency of 25 and 50 min. The

Table 2. Simulation results and limitations for various operational conditions.

Operation scenarios	Minimum catenary line voltage	Limitations for train operation
Nominal operation with 25 min headway	21.8 kV	25 min with 20 train
Nominal operation with 50 min headway	22.1 kV	50 min with 10 trains
Loss of first substation with 25 min headway	14 kV	$>$ 25 min or train limitation for that zone (10 trains)
Loss of first substation with 50 min headway	19.5 kV	50 min with 10 trains
Loss of second substation with 25 min headway	18 kV	$>$ 25 min or train limitation for that zone (10 trains)
Loss of second substation with 50 min headway	20 kV	50 min with 10 trains

worst state is losing the first transformer station at the trip frequency of 25 min, resulting in 14 kV minimum catenary voltage. The minimum catenary voltage values of the state of losing the first transformer station are lower than the values of the state of losing the second transformer station at the trip frequency of 25 and 50 min because of the long feeding region that was fed by the other transformer stations after the incident. As long as the catenary voltage remains within the limits permitted by the standard, the electrical losses decrease, and the power quality and vehicle performance increase. The simulation of the railway electrification system and traction power system is significant for system performance and efficiency.

Acknowledgment

This study is supported by the Controlled Project No. 33244 named "The Development of the Computer Supported Railway CER Simulation Program" of İstanbul University Scientific Research Projects Execution Secretary.

References

[1] Huh JS, Shin HS, Moon WS, Kang BW, Kim JC. Study on voltage unbalance improvement using SFCL in power feed network with electric railway system. IEEE T Appl Supercond 2013; 3: 3601004.

[2] Ghassemi A, Fazel SS, Maghsoud I, Farshad S. Comprehensive study on the power rating of a railway power conditioner using thyristor switched capacitor. IET Electr Syst Transport 2014; 4: 97-106.

[3] Raimondo G, Ladoux P, Lowinsky A, Caron H, Marino P. Reactive power compensation in railways based on AC boost choppers. IET Electr Syst Transport 2012; 2: 169-177.

[4] Aodsup K, Kulworawanichpong T. Effect of train headway on voltage collapse in high-speed AC railways. In: APPEEC 2012 Power and Energy Engineering Conference; 27–29 March 2012; Shanghai, China. New York, USA: IEEE. pp. 1-4.

[5] Baseri MAA, Nezhad MN, Sandidzadeh MA. Compensating procedures for power quality amplification of AC electrified railway systems using FACTS. In: PEDSTC 2011 Power Electronics Drive Systems and Technologies Conference; 16–17 February 2011; Tehran, Iran. New York, USA: IEEE. pp. 518-521.

[6] Brenna M, Foiadelli F. The compatibility between DC and AC supply of the Italian railway system. In: Power and Energy Society General Meeting; 24–29 July 2011; San Diego, CA, USA. New York, USA: IEEE pp. 1-7.

[7] Abrahamsson L, Kjellqvist T, Ostlund S. High-voltage DC-feeder solution for electric railways. IET Power Electron 2012; 5: 1776-1784.

[8] Raygani SV, Tahavorgar A, Fazel SS, Moaveni B. Load flow analysis and future development study for an AC electric railway. IET Electr Syst Transport 2012; 2: 139-147.

[9] Goodman CJ, Chymera M. Modelling and simulation. In: REIS 2013 Railway Electrification Infrastructure and Systems Conference; 3–6 June 2013; London, UK. New York, NY, USA: IEEE. pp. 16-25.

[10] Ladoux P, Raimondo G, Caron H, Marino P. Chopper-Controlled steinmetz circuit for voltage balancing in railway substations. IEEE T Power Electron 2013; 28: 5813-5822.

[11] Shin HS, Cho SM, Kim JC. Protection scheme using SFCL for electric railways with automatic power changeover switch system. IEEE T Appl Supercond 2012; 20: 5600604.

[12] Shin HS, Cho SM, Huh JS, Kim JC, Kweon DJ. Application on of SFCL in automatic power changeover switch system of electric railways. IEEE T Appl Supercond 2012; 22: 5600704.

[13] Kolar V, Hrbac R, Mlcak T. Measurement and simulation of stray currents caused by AC railway traction. In: EPE 2015 Electric Power Engineering Conference; 20–22 May 2015; Prague, Czech Republic. New York, USA: IEEE. pp. 764-768.

[14] Chen M, Jiang W, Luo J, Wen T. Modelling and simulation of new traction power supply system in electrified railway. In: ITSC 2015 IEEE 18th International Conference on Intelligent Transportation Systems; 15–18 September 2015; Las Palmas, Spain. New York, USA: IEEE. pp. 1345-1350.

[15] Soler M, Lopez J, Mera JM, Maroto J. Methodology for multiobjective optimization of the AC railway power supply system. IEEE T Intell Transp Syst 2015; 16: 2531-2542.

[16] He Z, Zhang Y, Gao S. Harmonic resonance assessment to traction power supply system considering train model in China high-speed railway. IEEE T Power Del 2014; 29: 1735-1743.

[17] Song W, Ma J, Zhou L, Feng X. Deadbeat predictive power control of single-phase three-level neutral-point-clamped converters using space-vector modulation for electric railway traction. IEEE T Power Electron 2016; 31: 721-732.

[18] Shafighy M, Khoo S, Kouzani AZ. Modelling and simulation of regeneration in AC traction propulsion system of electrified railway. IET Electr Syst Transport 2015; 5: 145-155.

[19] Kejian S, Mingli W, Agelidis VG, Hui W. Line current harmonics of three-level neutral point-clamped electric multiple unit rectifiers: analysis, simulation and testing. IET Power Electron 2014; 7: 1850-1858.

[20] Drabek P, Peroutka Z, Pittermann M, Cedl P. New configuration of traction converter with medium-frequency transformer using matrix converters. IEEE T Ind Electron 2011; 58: 5041-5048.

[21] Abrahamsson L, Kjellqvist T, Ostlund S. High-voltage DC-feeder solution for electric railways. IET Power Electron 2012; 5: 1776-1784.

[22] Tian Z, Hillmansen S, Roberts C, Weston P, Chen L, Zhao N, Su S, Xin T. Modeling and Simulation of DC Rail Traction Systems for Energy Saving. In: ITSC 2014 IEEE 17th International Conference on Intelligent Transportation Systems; 8–11 October 2014; Qingdao, China. New York, USA: IEEE. pp. 2354-2359.

[23] He J, Yu L, Wang X, Song X. Simulation of transient skin effect of DC railway system based on Matlab/Simulink. IEEE T Power Del 2013; 28: 145-152.

[24] Xu SY, Li W, Wang YQ. Effects of vehicle running mode on rail potential and stray current in DC mass transit systems. IEEE T Veh Technol 2013; 62: 3569-3580.

[25] Lao KW, Wong MC, Dai NY, Wong CK, Lam CS. Analysis of DC-link operation voltage of a hybrid railway power quality conditioner and its PQ compensation capability in high-speed cophase traction power supply. IEEE T Power Electron 2016; 31: 1643-1656.

[26] Takagi R, Preliminary evaluation of the energy-saving effects of the introduction of superconducting cables in the power feeding network for DC electric railways using the multi-train power network simulator. IET Electr Syst Transport 2012; 2: 103-109.

[27] Alamuti MM, Nouri H, Jamali S. Effects of earthing systems on stray current for corrosion and safety behaviour in practical metro systems. IET Electr Syst Transport 2011; 1: 69-79.

[28] Department of Railway Vehicle Management. Design Criteria of Hyundai-Rotem-Skoda E68000 Train. Ankara, Turkey: Turkish State Railways, 2016.